Werk

Jahr: 1981
Kollektion: fid.geo
Signatur: 8 Z NAT 2148:49
Digitalisiert: Niedersächsische Staats- und Universitätsbibliothek Göttingen
Werk Id: PPN1015067948_0049
PURL: http://resolver.sub.uni-goettingen.de/purl?PPN1015067948_0049

LOG Id: LOG_0020
LOG Titel: Temperature derivatives of compressional and shear wave velocities in crustal and mantle rocks at 6 kbar confining pressure
LOG Typ: article

Übergeordnetes Werk

Werk Id: PPN1015067948
PURL: http://resolver.sub.uni-goettingen.de/purl?PPN1015067948
OPAC: http://opac.sub.uni-goettingen.de/DB=1/PPN?PPN=1015067948

Contact

Niedersächsische Staats- und Universitätsbibliothek Göttingen
Georg-August-Universität Göttingen
Platz der Göttinger Sieben 1
37073 Göttingen
Germany
Email: gdz@sub.uni-goettingen.de

J. Geophys. 49, 47–56 (1981)

Journal of Geophysics

Temperature Derivatives of Compressional and Shear Wave Velocities in Crustal and Mantle Rocks at 6 kbar Confining Pressure

H. Kern and A. Richter

Mineralogisch-Petrographisches Institut der Universität Kiel, Olshausenstr. 40–60, D-2300 Kiel, Federal Republic of Germany

Abstract. Measurements of compressional and shear wave velocities, V_P and V_S, were made in a cubic anvil apparatus up to 700° C at 6 kbar in igneous and metamorphic rocks typical of the crust and mantle. Samples range in composition from acidic to ultramafic, with bulk density of 2.67–3.46 g/cm^3 at 6 kbar. Mean atomic weights of the rocks vary between 20.37 and 23.03. A rough dependence of wave velocity on bulk density is apparent. However, there is considerable scatter, and the velocities do not generally follow lines of constant mean atomic weight. Both V_P and V_S increase with increasing amphibole, garnet, pyroxene and olivine content. High quartz content produces relatively low *P*-wave and high *S*-wave velocities, giving significantly low Poisson's ratios. In contrast, a high feldspar content is related to relatively high *P*-wave and low *S*-wave velocities and consequent high Poisson's ratios. The calculated temperature derivatives of V_P and V_S for the range 20–500° C at 6 kbar confining pressure, using best-fit solutions, cover the range -1.60 to -4.94×10^{-4} km/s° C and -1.39 to -3.93×10^{-4} km/s° C, respectively. The results compare fairly well with the few data published so far. For the dunite and peridotite rocks the $(dV_P/dT)_p$-values are in excellent agreement with published Voigt-Reuss-Hill values calculated from single crystal data.

Using the experimental results, *P*-velocity profiles were calculated along a geotherm of a cold Precambrian shield crust and a warm continental crust. The temperature gradients for the latter cause velocity inversion in numerous rocks, rich in olivine or quartz.

Key words: High-temperature wave-velocities – Rock-sample wave-velocities – Velocity anisotropy.

Introduction

In recent years rapid progress has been made in the experimental determination of temperature derivatives of elastic wave velocities for natural rocks at pressures between 1 and 10 kbar and temperatures up to 750° C (Fielitz 1971; Kern and Fakhimi 1975; Stewart and Peselnick 1977, 1978; Ramananatoandro and Manghnani 1978; Christensen 1979; Kern 1978, 1979; Kern and Richter 1979). However, compared with the wealth of data about the pressure dependence of ultrasonic waves in rocks (Birch 1960, 1961; Simmons 1964; Christensen 1965, 1966, 1974), the literature about the influence of temperature at high confining pressure is scarce. There is a need for further investigations of the temperature dependence of compressional and shear wave velocities in crustal and mantle rocks. Elastic wave propagation through dry natural crystalline rocks are known to be sensitive to the state of microcracking of the material, in addition to its mineralogical composition. Therefore, only those measurements obtained at high confining pressure are valid for study of the influence of temperature.

We report here measurements compressional and shear wave velocities and the elastic constants of magmatic and metamorphic rocks typical of the crust and mantle. The metamorphic rocks chosen are representative of amphibolite and granulite facies conditions. The measurements were carried out at up to 700° C under a hydrostatic pressure of 6 kbar. Special attention is drawn to the relationship between mean velocities and the major mineral composition of the rocks.

Rock Samples

Fifteen samples which show a wide range of mineralogical and chemical composition (acidic to ultramafic) were selected for this study. Most of the metamorphic rocks were recovered from the metamorphic basement of Norwegian and Finnish Lappland. Sample number and locality, along with modal analyses are given in Table 1, where the samples are arranged in order of increasing density. Bulk densities were calculated using the weights and dimensions of the sample cubes. Chemical analyses of major oxides and the resultant mean atomic weights are presented in Table 2.

Experimental Technique

The seismic velocities have been measured by the ultrasonic transmission method in a cubic anvil apparatus designed for velocity measurements at high temperature T and high pressure p. Compressional and shear waves were generated by means of 2 MHz barium titanate transducers. Particulars of the device can be found in Kern and Fakhimi (1975).

A state of near hydrostatic stress is arrived at by advancing six pyramidal pistons in three mutually orthogonal directions onto cube shaped specimens. One end of each piston next to the specimen is surrounded by a furnace and heat is transmitted from the pistons to the specimens. Thus, a very homogenous temperature distribution is obtained within the large-volumed specimens. Temperature was measured using thermocouples placed in a cavity at the end of each piston, very close (about 1 mm) to the specimen. The temperature drop between the thermocouples and the center of the specimens is not more than 5° C at 700° C. Transducers are placed on the low temperature side of the pistons. The travel

0340-062X/81/0049/0047/$02.00

Table 1. Modal analyses (Percentages by volume)

Sample, No, locality	qu	mi	plg	or	hbl	gar	px	ep (zo)	ol	Others
Quartzite, 1452 Lam, Bayr. Wald, Germany	80	15	–	–	–	1	–	–	–	2 ctd 1 st
Bi-opx-plg-gneiss, 1400 Karasjok, Finnmark, Norway	15	3	66	–	–	–	13	–	–	2 ore 1 ap
Plg-amph-gneiss, 268 Karasjokka, Finnmark, Norway	33	–	40	–	24	1	–	–	–	1 ore 1 mi, cpx
Norite, 84 Radautal, Harz, Germany	1	1	57	–	8	–	28	–	–	5 sauss.
Px-plag-gar-gneiss, 1398 Karasjokka, Finnmark, Norway	33	–	40	–	3	16	5	–	–	2 ore
Amphibolite, 1387 S.-Alta, Finnmark, Norway	–	3	43	–	45	–	–	–	–	3 ore, 5 tit
Amphibolite, 1396 Karasjok, Finnmark, Norway	3	–	24	–	72	1	–	–	–	
Sill-gar-gneiss, 1403 Karasjok, Finnmark, Norway	24	–	6	25	–	27	–	–	–	14 sill, 1 rt
Plg-qu-amph-gneiss, 298 Karasjok, Finnmark, Norway	27	–	18	–	48	–	–	4	–	2 ore 1 tit
Ep-amphibolite, 1454 Hoher Bogen, Bayr. Wald, Germany	–	–	12	–	72	–	–	10	–	4 ser, 2 tit
Dunite, 1675 Aarheim, Norway	–	–	–	–	–	–	6	–	92	2 chl
Eclogite, 11 Münchberg, Fichtelgebirge, Germany	7	1	–	–	6	35	44	–	–	4 sympl. 2 rt
Ecoligte, 886c Saualpe, Austria	2	–	–	–	4	29	45	(10)	–	9 sympl 1 rt
Peridotite 475 Finero/Ivrea, Italy	–	–	–	–	–	–	15	–	80	3 serp 2 ore

Abbreviations: ap = apatite, bi = biotite, chl = chlorite, ctd = chloritoid, ep = epidote, gar = garnet, hbl = hornblende, mi = mica, ol = olivine, or = orthoclase, plg = plagioclase, px = pyroxene, qu = quartz, rt = rutile, sauss = saussurite, ser = sericite, serp = serpentinite, sill = sillimanite, st = staurolite, sympl = symplecitite, tit = titanite, zo = zoisite

Table 2. Major oxide analyses (wt.%) and mean atomic weights ($\bar{m}$). Analyst: P.K. Hörmann

	1452	1400	268	84	1398	1387	1396	1403	298	1454	1675	11	886
SiO_2	89.46	63.01	66.91	50.40	64.82	51.87	47.40	56.30	49.73	47.60	41.14	50.24	48.54
Al_2O_3	6.36	16.70	14.55	18.14	14.89	13.80	13.71	23.95	14.83	14.84	2.20	13.60	15.05
TiO_2	0.12	0.67	0.35	0.24	0.47	1.84	1.13	0.92	1.23	0.97	0.004	2.04	1.12
Fe_2O_3	0.92	1.87	2.32	0.56	1.84	6.19	3.00	1.13	5.31	3.70	1.10	4.72	2.65
FeO	1.21	3.37	3.96	4.64	6.18	7.17	9.43	8.55	8.45	6.07	5.34	9.05	5.82
MnO	0.026	0.079	0.120	0.129	0.182	0.139	0.201	0.088	0.237	0.021	0.088	0.249	0.145
MgO	0.08	3.15	1.93	8.69	1.95	4.19	9.35	3.90	4.78	7.83	48.03	6.46	8.82
CaO	0.02	5.34	6.12	13.06	7.06	7.45	11.10	0.72	10.77	13.82	0.09	9.67	13.67
Na_2O	0.03	3.35	3.15	1.77	2.11	4.84	2.71	0.90	2.66	2.69	0.06	3.11	3.04
K_2O	0.93	1.85	0.63	0.17	0.25	1.00	0.46	2.65	0.43	0.23	0.02	0.13	0.03
P_2O_5	0.051	0.242	0.089	0.010	0.172	0.126	0.123	0.048	0.084	0.081	0.002	0.249	0.072
H_2O^+	0.80	0.57	0.19	1.20	0.42	0.96	1.68	0.47	1.16	1.97	0.89	0.74	0.49
H_2O^-	0.07	0.14	0.08	0.39	0.10	0.06	0.08	0.13	0.08	0.15	0.11	0.11	0.07
CO_2	0.04	0.16	0.02	0.09	0.04	0.05	0.28	0.16	0.10	0.06	0.07	0.05	0.01
$\Sigma =$	100.12	100.50	100.42	99.49	100.48	99.69	100.65	99.92	99.85	100.03	99.14	100.42	99.53
$\bar{m} =$	20.37	21.55	21.65	21.67	21.97	22.63	22.88	21.94	22.90	20.26	20.78	23.03	22.37

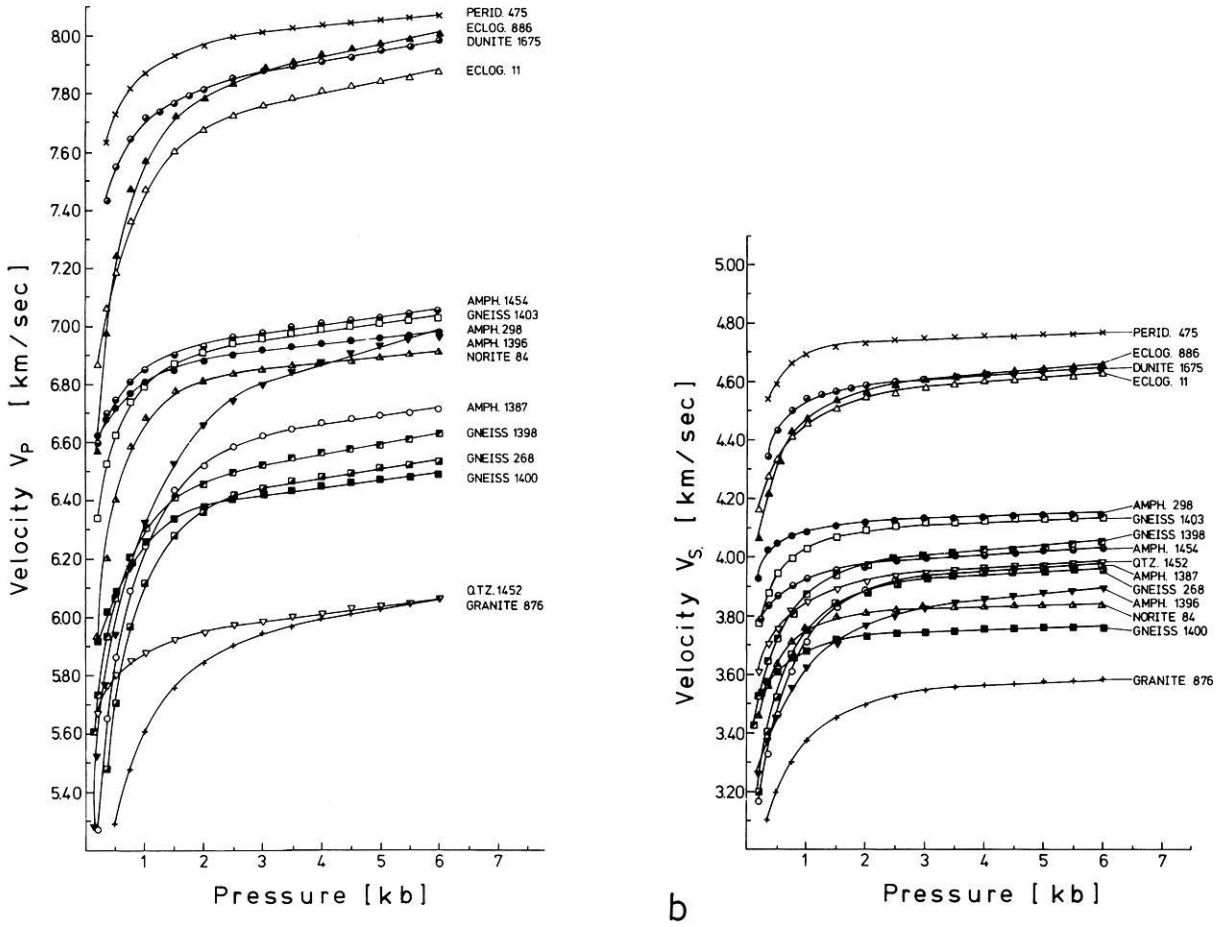

Fig. 1a and b. Velocities of (**a**) compressional waves and (**b**) shear wave as a function of pressure at room temperature. V_P is the mean of the velocities measured in the three orthogonal directions (x,y,z) of the sample cubes, V_S is the velocity in the x direction

time of the pulses through the specimens is obtained by subtracting the calibrated time needed for the pulse to travel to and from the specimen through the pistons from the total time measured by the transducers.

The experiments were carried out on rock cubes (43 mm on edge) cut from larger blocks, free of macroscopic fractures and secondary alteration. Edges of the sample cubes were parallel to visible macroscopic fabric directions (foliation, banding). The compressional wave velocity was measured simultaneously in the three orthogonal directions (x, y, z) of the cubes to obtain information on the directional dependence of the wave velocities. In one direction (x) the velocities of compressional and shear waves were measured at the same time. In general the x direction was normal to foliation or banding. The travel time was determined with a digital counter by comparing the output and input impulses on a dual-trace oscilloscope. The precision of timing measurements is ± 5 ns, and the timing accuracy is believed to better than $\pm$ 0.5%.

Wave velocities were measured at about 0.5 kbar intervals during the pressure increase to 6 kbar. Maintaining the hydrostatic pressure of 6 kbar, the temperature was increased in steps of about 50°–80° C over 30-min periods. To ensure that the samples had reached pressure and temperature equilibrium, successive readings were taken at time intervals of at least 40 min.

Results and Discussion

All the measurements described above were obtained from runs on fresh cubes of rocks. In general, the data presented were obtained from specimens compressed and heated for the first time. To check reversibility, velocities for two specimens were measured during heating as well as during cooling. A correction for the change of length of the specimens with pressure and temperature, was applied to the calculation of velocity.

The pressure and temperature dependence of wave velocities and the respective dynamic elastic parameters of polycrystalline rocks depend on two factors: (1) the pressure and temperature sensitivity of the elastic parameters of the constituent minerals and (2) on the state of microfracturing of the material.

Relations Between Velocity, Density, Chemistry, and Mineralogy at Room Temperature

The pressure dependence of V_P and V_S at room temperature is shown in Fig. 1. The velocity curves were obtained from measurements made while raising pressure to the 6 kbar confining pressure being applied for the velocity measurements at high temperatures. The general velocity increase with pressure may be attributed to

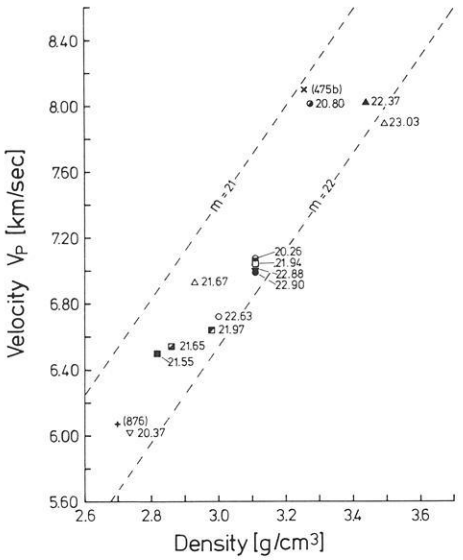

Fig. 2. Compressional wave velocities versus density at 6 kbar confining pressure. The numbers attached to *symbols* are mean atomic weights (Table 2). *Dashed lines* represent lines of constant mean atomic weight, according to Birch (1961)

compaction of pore space, in particular the closing of microcracks. Above about 2 kbar the velocity-pressure relations tend to become linear, indicating the intrinsic effect of pressure on wave velocities.

In Fig. 2 mean values of V_P are plotted against density. The numbers attached to the symbols represent mean atomic weights (Table 1). Also shown are the mean atomic weight lines, $m=21$ and $m=22$, as determined for compressional wave velocities by Birch (1961). The mean atomic weights of the rocks investigated vary between 20.37 (acidic) and 23.03 (mafic). As already shown by Birch (1961), differences in mean atomic weights of rocks are primarily related to iron and titanium content – the higher their content, the higher is the mean atomic weight (see also Table 1).

A rough dependence of wave velocities on bulk density is apparent. However, there is considerable scatter and the velocities in general do not follow lines of constant mean atomic weight. This partially irregular behavior can be explained by the mineralogical complexities. In Fig. 3 comparison is made between the percentages of major minerals and the compressional and shear wave velocities at 6 kbar confining pressure. From this it is evident that velocities are closely related to the percentages of major minerals in rocks and the respective single crystal velocities. In general, high contents of olivine, garnet, pyroxene and amphibole produce high compressional and shear wave velocities. Increasing quartz

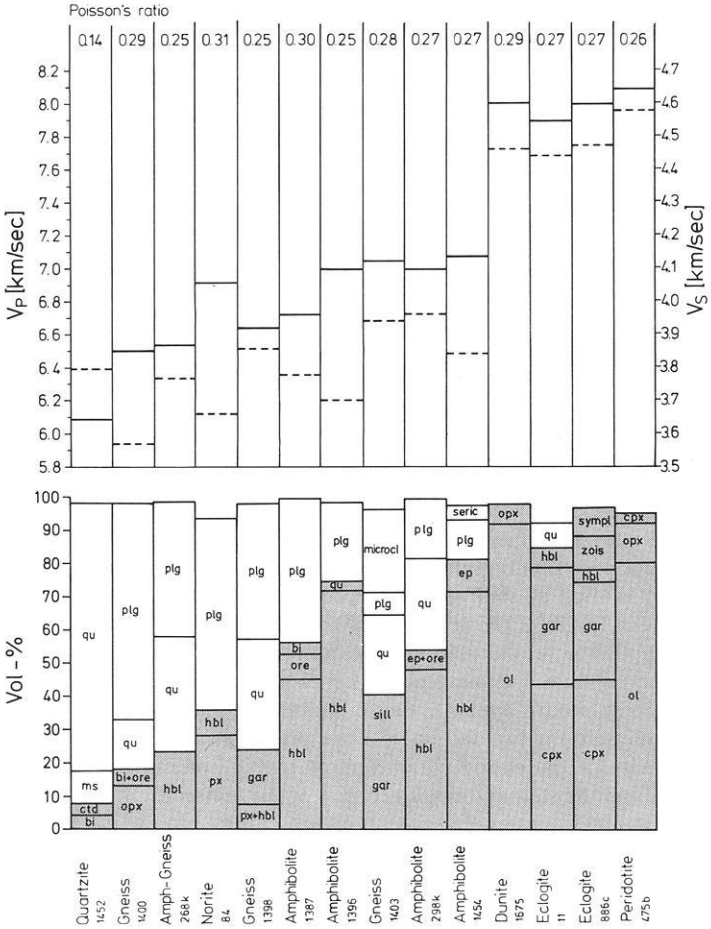

Fig. 3. Comparison between the percentages of major minerals and compressional wave velocities, shear wave velocities, and Poisson's ratio at 6 kbar confining pressure. For abbreviations see Table 3. The samples are arranged in order of increasing density (except 475). The *dark shaded areas* represent the dark minerals with generally high single crystal velocities. *Solid bars* (upper diagram) refer to V_P, *dashed* to V_S

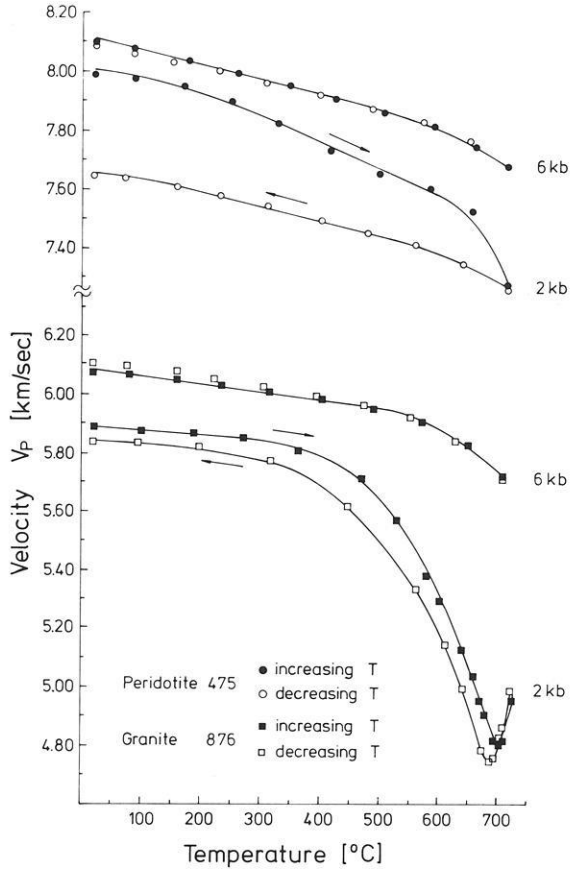

Fig. 4. Compressional wave velocities for peridotite 475 and granite 876 as a function of temperature at 2 kbar and 6 kbar confining pressure. *Solid symbols* indicate measurements with increasing temperature; *open symbols* indicate measurements with decreasing temperature. The velocity inversion in granite at 2 kbar is caused by the high-low transition in the constituent quartz minerals

content (samples No. 1398, 268 1452) results in a decrease of V_P and an accompanying increase in V_S, thereby significantly lowering Poission's ratio (Table 4). Compared to most major rock-forming silicates, quartz has an extremely low Poisson's ratio (Christensen and Fountain 1975; Kern 1979). On the other hand, high feldspar contents produce relatively low shear velocities and high Poisson's ratio (samples No. 84 and 1400).

Velocity-Temperature Relations at 6 kbar Confining Pressure

At a given pressure differential thermal expansion of the constituent minerals of rocks may cause grain boundary cracks to widen and new cracks to open. However, the microfracturing induced by the rapid thermal change of volume of the mineral phases will be more and more suppressed with increasing confining pressure and microfracturing should have little effect at pressures of a few kilobars. As was shown earlier (Kern 1978), the minimum pressure needed to prevent damage seems to be about 1 kbar per 100° C. The arguments borne out by that paper are substantiated by the observations on two cycled samples of granite and periodotite (Fig. 4). At 2 kbar confining pressure non-linear slope and significant hysteresis is observed on the velocity-temperature curves, indicating microfracturing. At 6 kbar confining pressure, however, the slope is near linear and reversibility is obtained on both plots. Thus, the values obtained under these conditions are considered to be the most nearly correct intrinsic properties of the compact aggregates. Therefore, in order to determine the temperature derivatives of velocities, the measurements of V_P and V_S were carried out under confining pressure conditions of 6 kbar.

V_P and V_S as a function of temperature at 6 kbar are presented in Fig. 5a–b. The data show that the decrease of *P*-and *S*- wave velocities is almost linear as temperature is increased from room value up to about 500° C. However, there is a significant decrease in the slope beyond this temperature, and the velocity-temperature curves become highly non-linear, indicating the onset of thermal cracking.

It should be noted, that a velocity minimum due to the high-low quartz transition (compare Fig. 4) is not observed on the velocity curves of the quartz-bearing rocks at 6 kbar. The pressure dependence and the shift of the α–β quartz transition temperature in polycrystalline aggregates (Kern 1978, 1979) places the transition temperature outside the temperature range investigated.

The best-fit solutions of the velocity-pressure and velocity-temperature data using the equations

$$V_P(p,T) = V_{P_0} + (dV_P/dp)_T \cdot p + (dV_P/dT)_p \cdot T$$

and

$$V_S(p,T) = V_{S_0} + (dV_S/dp)_T \cdot p + (dV_S/dT)_p \cdot T$$

are given in Table 3.

The pressure derivatives refer to 2–6 kbar at room temperature and the temperature derivatives to 20° C–500° C at 6 kbar confin-

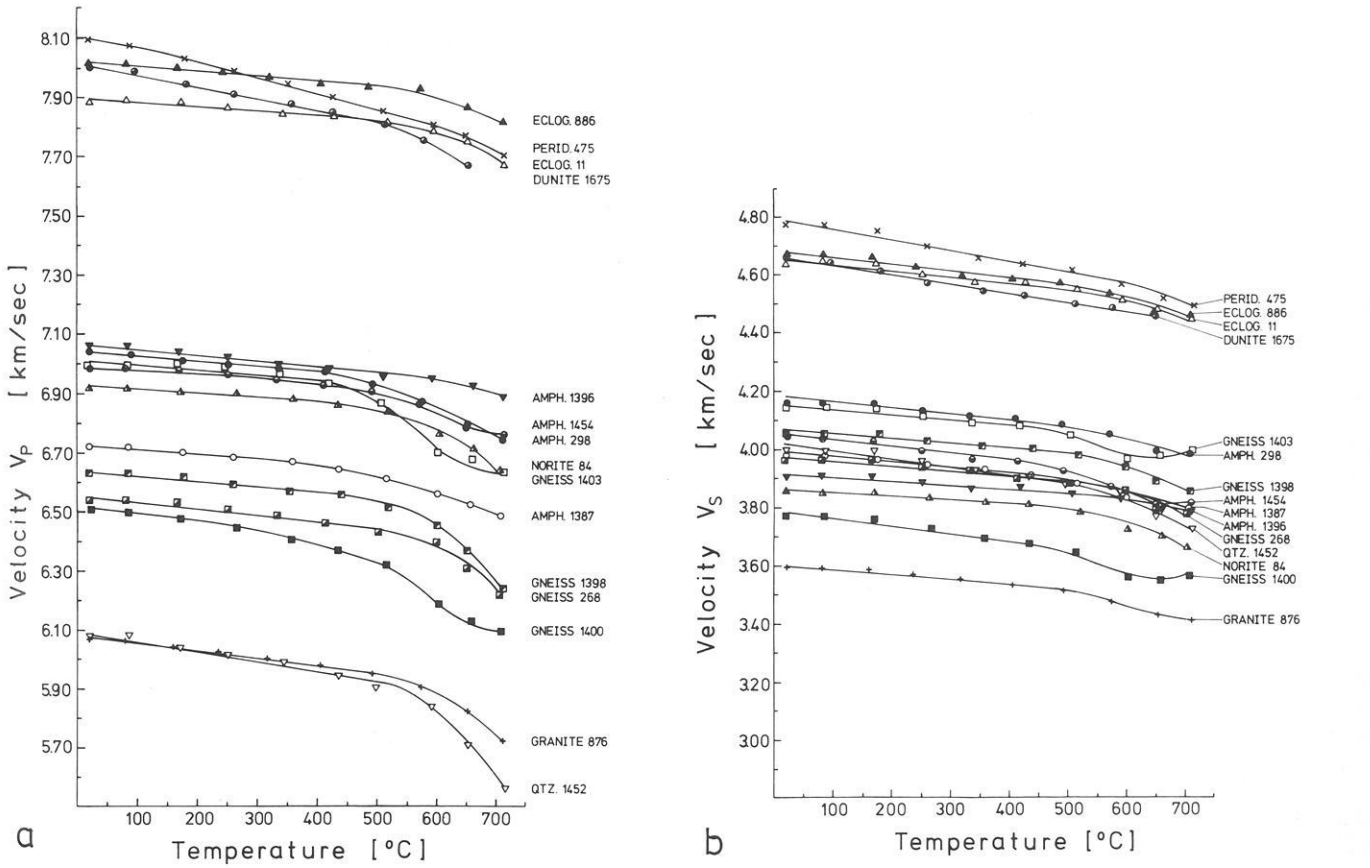

Fig. 5a and b. Velocities of (**a**) compressional waves and (**b**) shear waves for the different rock types as a function of temperature at 6 kbar confining pressure. V_P is the mean of the velocities measured in three orthogonal directions of the sample cubes, V_S is the velocity in one direction

Table 3. Pressure and temperature derivatives of *P*- and *S*-waves velocities of various rocks
V_P is the mean of the velocites measured in the three orthogonal directions of the sample cubes, V_S is the velocity in one direction
The reference state $V = V_0$ is 0 kbar and 0° C

Rock type/ Sample No.		V_{P_0} V_{S_0} (km × s^{-1})	$dV_P/dp \times 10^2$ $dV_S/dp \times 10^2$ (km × s^{-1} kbar^{-1})	$-dV_P/dT \times 10^4$ $-V_S/dT \times 10^4$ (km × s^{-1}°C^{-1})
Quartzite	V_P	5.905 ± 0.004	2.94 ± 0.1	4.01 ± 0.3
1452	V_S	3.910 ± 0.004	1.46 ± 0.08	2.85 ± 0.3
Bio-cpx-plg-gneiss	V_P	6.360 ± 0.006	2.42 ± 0.1	4.78 ± 0.3
1400	V_S	3.727 ± 0.003	0.84 ± 0.08	2.85 ± 0.2
Cpx-plg-gar-gneiss	V_P	6.420 ± 0.007	3.67 ± 0.2	2.46 ± 0.2
1398	V_S	3.964 ± 0.004	1.60 ± 0.09	1.70 ± 0.2
Amph-plg-gar-gneiss	V_P	6.339 ± 0.01	3.56 ± 0.3	2.51 ± 0.2
268	V_S	3.884 ± 0.006	1.49 ± 0.1	2.01 ± 0.2
Sill-gar-gneiss	V_P	6.871 ± 0.01	3.03 ± 0.2	3.61 ± 0.3
1403	V_S	4.091 ± 0.003	1.01 ± 0.07	2.22 ± 0.2
Amphibolite	V_P	6.516 ± 0.01	3.63 ± 0.3	2.37 ± 0.2
1387	V_S	3.885 ± 0.006	1.68 ± 0.1	2.08 ± 0.2
Amphibolite	V_P	6.610 ± 0.02	6.59 ± 0.50	0.72 ± 0.2
1936	V_S	3.746 ± 0.01	2.79 ± 0.2	1.39 ± 0.2
Ep-amphibolite	V_P	6.905 ± 0.005	2.80 ± 0.1	2.99 ± 0.2
1454	V_S	3.965 ± 0.003	1.27 ± 0,06	2.65 ± 0.2
Amphibolite	V_P	6.857 ± 0.005	2.28 ± 0.1	2.02 ± 0.2
298	V_S	4.109 ± 0.003	0.92 ± 0.06	1.81 ± 0.2
Eclogite	V_P	7.641 ± 0.01	4.17 ± 0.2	1.60 ± 0.2
11	V_S	4.535 ± 0.006	1.73 ± 0.1	2.11 ± 0.3
Eclogite	V_P	7.740 ± 0.01	4.75 ± 0.3	1.86 ± 0.1
886c	V_S	4.548 ± 0.006	2.09 ± 0.1	2.48 ± 0.2
Norite	V_P	6.770 ± 0.005	2.58 ± 0.1	1.73 ± 0.2
84	V_S	3.803 ± 0.003	0.94 ± 0.07	1.49 ± 0.1
Dunite	V_P	7.772 ± 0.004	3.73 ± 0.1	4.12 ± 0.1
1675	V_S	4.566 ± 0.004	1.59 ± 0.09	3.54 ± 0.2
Granite	V_P	5.818 ± 0.01	4.37 ± 0.3	2.69 ± 0.1
876	V_S	3.496 ± 0.008	1.79 ± 0.1	2.08 ± 0.1
Peridotite	V_P	7.949 ± 0.007	2.36 ± 0.2	4.94 ± 0.2
475	V_S	4.721 ± 0.002	0.946 ± 0.07	3.93 ± 0.3

ing pressure. The computed coefficients cover the range 2.28–6.59×10^{-2} km/s kbar for compressional wave velocities and 0.84–2.79×10^{-2} km/s kbar for shear wave velocities. The temperature derivatives range from -1.6 to -4.94×10^{-4} km/s °C for compressional wave velocities and from -1.39 to -3.93×10^{-4} km/s °C for shear wave velocities. The resulting temperature coefficients of V_P and V_S are in general largest in quartz-bearing and olivine-bearing rocks.

Because experimental work on temperature derivatives for crustal and mantle rocks under conditions of high confining pressure is still scarce, only limited camparisons can be made with published data. Comprehensive temperature data for V_P for a wide variety of igneous and metamorphic rocks (Christensen 1979) came to the attention of these authors as this manuscript was being submitted. Christensen estimated temperature coefficients at 2 kbar confining pressure up to 500° C. Because of the relatively low confining pressure, the velocity is an approximately linear function below 300° C only, thus indicating intrinsic behavior only within this temperature range. The T derivatives of V_P at higher temperatures are believed to be influenced by grain boundary openings. In general, Christensen's values are a little larger than our own for rocks of comparable composition.

For dunite we obtained a $(dV_P/_P/dT)_p$-value of -4.12×10^{-4} km/s °C. Christensen estimated -5.6×10^{-4} km/s °C, while Ramananantoandro and Manghnani (1978) measured a mean of -6.1×10^{-4} km/s °C for an anisotropic dunite at 10 kbar, for the range 25°–500° C. Peselnick and Nicolas (1978) measured T derivatives of V_P in a harzburgite and Iherzolite rock for the range 20°–250° C at 8 kbar confining pressure. The results for the two rocks are approximately the same (-6×10^{-4} to -7×10^{-4} km/s °C) and are again a little larger than our value for a peridotite rock (-4.94×10^{-4} km/s °C).

Our experimental data for dunite and peridotite (80% olivine by volume), however, compare fairly well with T derivatives of V_P calculated from single crystal data using the Voigt-Reuss-Hill assumption. Kumazawa and Anderson (1969) calculated -4.95×10^{-4} km/s °C for an isotropic aggregate of olivine and Ramananantoandro and Manghnani (1978) calculated -4.4×10^{-4} to -4.6×10^{-4} km/s °C for three anisotropic dunite cores.

For eclogites we measured significantly smaller temperature coefficients of V_P(-1.6×10^{-4} to -1.86×10^{-4} km/s °C) than Christensen ($-5.3 \cdot 10^{-4}$ km/s °C). Better agreement was obtained in quartz-bearing rocks. For granite, granulitegneiss and quartzite we obtained temperature derivatives of V_P between -2.69×10^{-4} and -4.1×10^{-4} km/s °C. Christensen obtained temperature coefficients ranging from -3.9×10^{-4} to -5.4×10^{-4} km/s °C for the

Table 4. V_{P_x}, V_{S_x} and elastic constants for selected temperatures at 6 kbar (for explanation of symbols see text)

Rocktype Sample No.	T (°C)	ρ (g/cm^3)	V_{P_x} (km/s)	V_{S_x} (km/s)	V_{P_x}/V_{S_x}	σ	ϕ (km^2/s^2)	K (Mbar)	β (Mbar^{-1})	G (Mbar)	E (Mbar)	λ (Mbar)
Granite	20	2.701	5.989[a]	3.397	1.763	0.262	20.48	0.553	1.807	0.311	0.787	0.345
876	160	2.695	5.955	3.383	1.760	0.261	20.20	0.544	1.836	0.308	0.778	0.338
$A=2.0\%$	315	2.693	5.911	3.346	1.766	0.264	20.01	0.538	1.855	0.301	0.762	0.337
	490	2.690	5.872	3.304	1.777	0.268	19.92	0.535	1.865	0.293	0.744	0.340
	710	2.667	5.648	3.201	1.764	0.263	18.23	0.486	2.055	0.273	0.690	0.304
Quartzite	20	2.735	5.883[b]	3.800	1.548	0.142	15.35	0.419	2.380	0.394	0.902	0.156
1452	170	2.733	5.849	3.796	1.540	0.136	14.99	0.409	2.439	0.393	0.894	0.147
$A=6.0\%$	340	2.726	5.763	3.723	1.547	0.141	14.73	0.401	2.490	0.377	0.862	0.149
	500	2.711	5.680	3.674	1.545	0.140	14.26	0.386	2.585	0.365	0.834	0.142
	710	2.680	5.337	3.520	1.516	0.115	11.96	0.320	3.119	0.332	0.740	0.099
Gneiss	20	2.816	6.578[c]	3.574	1.840	0.290	26.23	0.738	1.353	0.359	0.928	0.499
1400	170	2.817	6.532	3.556	1.836	0.289	25.80	0.726	1.375	0.356	0.918	0.489
$A=2.4\%$	360	2.815	6.442	3.489	1.846	0.292	25.26	0.711	1.405	0.342	0.885	0.482
	515	2.810	6.340	3.436	1.845	0.292	24.45	0.687	1.455	0.331	0.857	0.465
	710	2.801	6.103	3.362	1.815	0.282	22.17	0.621	1.609	0.316	0.811	0.410
Amphibole	20	2.857	6.499[a]	3.769	1.724	0.246	23.29	0.665	1.502	0.405	1.011	0.395
Gneiss	170	2.860	6.481	3.769	1.719	0.244	23.06	0.659	1.516	0.406	1.011	0.388
268	335	2.860	6.423	3.726	1.723	0.246	22.74	0.650	1.537	0.397	0.989	0.385
$A=1.5\%$	505	2.854	6.371	3.679	1.731	0.249	22.54	0.643	1.554	0.386	0.965	0.385
	710	2.832	6.136	3.572	1.717	0.243	20.63	0.584	1.710	0.361	0.898	0.343
Norite	20	2.930	6.976[c]	3.658	1.907	0.310	30.82	0.903	1.107	0.392	1.027	0.641
84	170	2.934	6.958	3.648	1.907	0.310	30.66	0.899	1.111	0.390	1.023	0.639
$A=1.6\%$	360	2.935	6.926	3.611	1.918	0.313	30.58	0.897	1.114	0.382	1.005	0.642
	520	2.929	6.870	3.580	1.918	0.313	30.10	0.881	1.133	0.375	0.986	0.631
	700	2.918	6.678	3.454	1.933	0.317	28.68	0.837	1.194	0.348	0.917	0.605
Gneiss	20	2.976	6.644[a]	3.858	1.722	0.245	24.29	0.723	1.382	0.442	1.103	0.427
1398	180	2.980	6.625	3.856	1.718	0.243	24.06	0.717	1.394	0.443	1.102	0.421
$A=0.8\%$	350	2.978	6.571	3.810	1.724	0.246	23.82	0.709	1.409	0.432	1.077	0.421
	520	2.967	6.520	3.777	1.726	0.247	23.48	0.696	1.434	0.423	1.056	0.414
	710	2.946	6.256	3.649	1.714	0.242	21.38	0.629	1.587	0.392	0.974	0.368
Amphibolite	20	2.999	7.041[c]	3.778	1.863	0.297	30.54	0.916	1.091	0.428	1.111	0.630
1387	175	2.999	7.026[a]	3.761	1.868	0.299	30.50	0.914	1.093	0.424	1.102	0.632
$A=8.0\%$	360	3.001	6.991	3.724	1.877	0.301	30.38	0.911	1.096	0.416	1.083	0.634
	515	2.995	6.935	3.673	1.888	0.305	30.10	0.901	1.109	0.404	1.054	0.632
	710	2.976	6.809	3.586	1.898	0.308	29.21	0.869	1.150	0.382	1.001	0.614
Amphibolite	20	3.106	6.471[a]	3,711	1.743	0.254	23.51	0.730	1.369	0.427	1.073	0.445
1396	170	3.111	6.455	3.709	1.740	0.253	23.32	0.725	1.378	0.427	1.072	0.440
$A=11.0\%$	335	3.114	6.406	3.666	1.747	0.256	23.11	0.719	1.389	0.418	1.051	0.440
	510	3.109	6.355	3.646	1.743	0.254	22.66	0.704	1.419	0.413	1.037	0.429
	710	3.087	6.270	3.580	1.751	0.258	22.22	0.686	1.457	0.395	0.995	0.422
Gneiss	20	3.107	7.155[c]	3.949	1.811	0.280	30.40	0.944	1.058	0.484	1.241	0.621
1403	175	3.108	7.121	3.938	1.808	0.279	30.03	0.933	1.071	0.481	1.233	0.612
$A=3.3\%$	340	3.106	7.054	3.888	1.814	0.281	29.60	0.919	1.087	0.469	1.203	0.606
	505	3.099	6.957	3.844	1.809	0.280	28.69	0.889	1.124	0.457	1.172	0.584
	710	3.081	6.741	3.798	1.774	0.267	26.20	0.807	1.238	0.444	1.126	0.511
Amphibolite	20	3.107	7.077[b]	3.961	1.786	0.271	29.16	0.906	1.103	0.487	1.240	0.581
298	170	3.109	7.065	3.958	1.784	0.271	29.02	0.902	1.108	0.487	1.238	0.577
$A=4.8\%$	330	3.107	7.019	3.910	1.795	0.275	28.88	0.897	1.114	0.475	1.211	0.580
	490	3.102	6.970	3.882	1.795	0.275	28.48	0.883	1.131	0.467	1.192	0.572
	710	3.082	6.793	3.777	1.798	0.276	27.12	0.835	1.196	0.439	1.122	0.542
Amphibolite	20	3.109	6.885[a]	3.842	1.792	0.273	27.72	0.861	1.160	0.458	1.169	0.555
1454	170	3.107	6.853	3.822	1.793	0.274	27.48	0.854	1.170	0.453	1.156	0.551
$A=6.0\%$	335	3.109	6.781	3.759	1.803	0.278	27.14	0.843	1.185	0.439	1.123	0.550
	490	3.102	6.712	3.718	1.805	0.278	26.61	0.825	1.211	0.428	1.096	0.539
	710	3.084	6.515	3.614	1.802	0.277	25.03	0.771	1.295	0.402	1.029	0.503
Dunite	20	3.278	8.227[c]	4.462	1.843	0.291	41.13	1.348	0.741	0.652	1.685	0.913
1675	180	3.280	8.163	4.408	1.851	0.294	40.72	1.335	0.748	0.637	1.649	0.910
$A=4.8\%$	355	3.271	8.072	4.337	1.861	0.297	40.07	1.310	0.762	0.615	1.596	0.900
	510	3.261	8.022	4.292	1.869	0.299	39.79	1.297	0.770	0.600	1.561	0.897
	710	3.271	7.925	4.291	1.846	0.292	38.25	1.251	0.799	0.602	1.557	0.849

Continuation on p. 54

Table 4 (continued)

Rocktype Sample No.	T (°C)	ρ (g/cm^3)	V_{P_x} (km/s)	V_{S_x} (km/s)	V_{P_x}/V_{S_x}	σ	ϕ (km^2/s^2)	K (Mbar)	β (Mbar^{-1})	G (Mbar)	E (Mbar)	λ (Mbar)
Eclogite	20	3.495	7.886[b]	4.438	1.776	0.268	35.92	1.255	0.796	0.688	1.746	0.796
11	175	3.499	7.880	4.436	1.776	0.268	35.85	1.254	0.797	0.688	1.746	0.795
$A=0.3\%$	340	3.496	7.822	4.372	1.789	0.272	35.69	1.247	0.801	0.668	1.701	0.802
	515	3.488	7.783	4.346	1.790	0.273	35.39	1.234	0.810	0.658	1.677	0.795
	710	3.463	7.622	4.242	1.796	0.275	34.10	1.180	0.846	0.623	1.589	0.765
Ecologite	20	3.442	7.975[c]	4.470	1.784	0.270	36.95	1.272	0.786	0.687	1.748	0.813
886	170	3.443	7.954	4.457	1.784	0.271	36.77	1.266	0.789	0.683	1.738	0.810
$A=0.8\%$	320	3.437	7.893	4.395	1.795	0.275	36.54	1.256	0.796	0.663	1.693	0.813
	485	3.435	7.863	4.365	1.801	0.277	36.42	1.251	0.799	0.654	1.671	0.814
	710	3.409	7.730	4.256	1.816	0.282	35.60	1.213	0.823	0.617	1.583	0.801
Peridotite	20	3.290	8.010[b]	4.575	1.750	0.257	36.25	1.192	0.838	0.688	1.732	0.733
475	180	3.288	7.955	4.543	1.751	0.258	35.76	1.175	0.850	0.678	1.707	0.723
$A=4.7\%$	350	3.282	7.842	4.448	1.763	0.262	35.11	1.152	0.867	0.649	1.640	0.719
	510	3.272	7.733	4.404	1.755	0.259	33.93	1.110	0.900	0.634	1.599	0.687
	715	3.259	7.474	4.280	1.746	0.256	31.43	1.024	0.976	0.596	1.499	0.626

V_{P_x} and V_{S_x} are velocities in the x direction of the sample coordinates

[a] Lowest velocity in the anisotropic aggregates
[b] Intermediate
[c] Highest
[d] In this run the x direction of the sample coordinates is parallel to the foliation

same rocks. Our results for quartz-bearing granite and gneiss rocks are almost within the range of values reported by Spencer and Nur (1976) for Westerly granite (-1×10^{-4} to -5×10^{-4} km/s °C) heated to 400° C at 5 kbar confining pressure.

To our knowledge, temperature coefficients of V_S have not yet been published, so that no comparison is possible.

In general, the temperature derivatives of V_S are smaller than those of V_P except for eclogites and amphibolites (Table 3). In both eclogite samples V_S decreases significantly more than V_P with increasing temperature. In amphibolites the temperature coefficients of V_S equal, more or less, those of V_P or are a little larger.

Velocity Anisotropy

Significant velocity anisotropies

$$A=\frac{V_{\max}-V_{\min}}{V_{\max}}\times 100\%$$

were measured in peridotite, dunite, amphibolite and quartzite rocks. The directional dependence of elastic wave velocities is at least a result of both (1) preferred lattice orientation of minerals and (2) microcracks which are preferrently orientated parallel to grain boundaries. As was shown by Kern (1978) the part of the velocity anisotropy that may be attributed to oriented cracks is eliminated at higher confining pressure. Therefore, the velocity anisotropies for 6 kbar confining pressure listed in Table 4 must be due to preferred lattice orientation of constituent minerals. Petrofabric analyses with the X-ray goniometer (amphibolite) and the universal stage (dunite, peridotite, quarzite) show significant preferred lattice orientation of dominant minerals (i.e., hornblende, olivine, quartz, mica) in these rocks, and this part of the elastic anisotropy is unavvected by temperature even at 700° C.

Dynamic Elastic Parameters at High Pressure and Temperature

Compressional and shear wave velocities measured simultaneously in one sample direction at 6 kbar confining pressure are given in Table 4 for various temperatures, together with the values of the compressional to shear velocity ratio (V_P/V_S), Poisson's ratio (σ), the seismic parameter (ϕ), the bulk moduls (K), the compressibility (β), the shear moduls (G), Young's modulus (E), and the Lamé's constant (λ) as calculated from measured densities and velocities. The dynamic elastic parameters for significantly anisotropic samples must be treated with caution because the elastic constants were calculated by use of the formulas proposed by Birch (1960) for isotropic bodies.

In general, the values of K, G, E, and ϕ at high confining pressure show a decrease with temperature. It should be noted that in quartz-bearing rocks the bulk moduls decreases much more than the shear moduls.

Application to Geology and Geophysics

The quasi-linearity of the velocity-pressure relations between 2 and 6 kbar at room temperature and of the velocity-temperature relations at 6 kbar in the range 20°–500° C for the rocks investigated (Fig. 5) suggest that calculated pressure and temperature derivatives approach those of pore-free aggregates. It should be noted, however, that our measurements were carried out on dry samples and it is well established that pore fluids may affect compressional

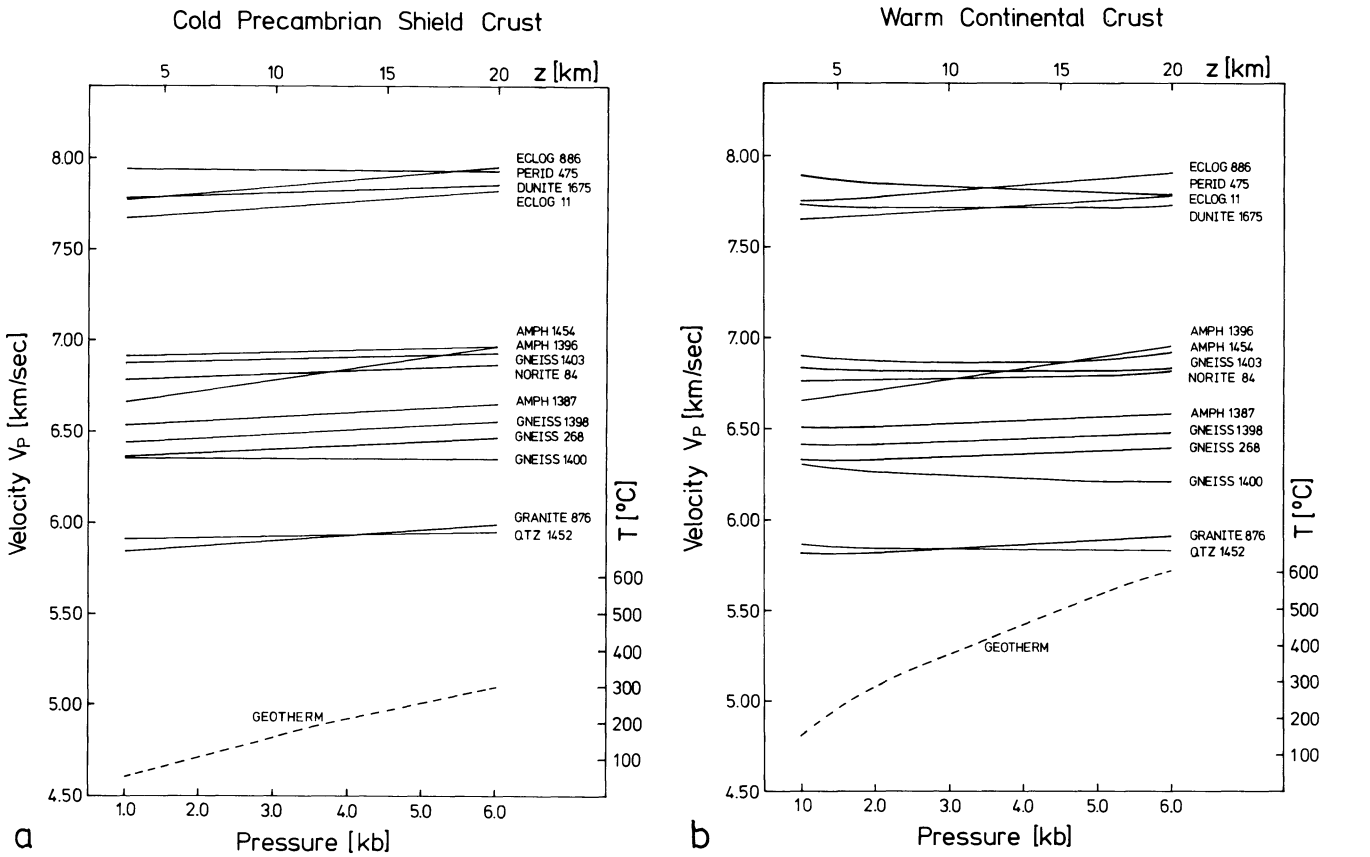

Fig. 6a and b. Compressional wave velocities for different rock types under pressure and temperature conditions of **a** a cold Precambrian shield and **b** a warm continental crust geotherm. The assumed geotherms (after Theilen and Meissner, 1979) are shown by the *bottom curve*

wave velocities (Nur and Simmons 1969; Spencer and Nur 1976). Crustal and mantle igneous and high-grade metamorphic rocks, however, are in general water-depleted. Therefore, at deeper crustal levels, pore fluid pressure may be very small and the effective pressure nearly identical to the lithostatic pressure.

On the basis of this assumption we used our experimentally determined pressure and temperature derivatives of the mean values of V_P to calculate velocity-depth profiles. In Fig. 6 we have plotted *P*-velocities of different rocks for a cold Precambrian shield crust (a) and for a warm continental crust (b). The computation is based on geotherms (bottom curve) reported by Theilen and Meissner (1979).

Along the geotherm of a Precambrian shield crust (a) the velocity function increases with depth for all rocks investigated (except for the peridotite rock), but the rate of velocity increase may be different from rock type to rock type. The temperature gradients valid for a warm continental crust (b), however, cause a velocity inversion in numerous rocks. As is evident from Fig. 6b the velocity-depth relations show small negative velocity gradients for olivine-bearing rocks and less significantly for quartz-bearing rocks (gneiss, quartzite), due to the temperature sensitivity of wave velocity in olivine and quartz single crystals.

This observation is compatible with results from deep seismic sounding, which indicate that large velocity reversals are not found in the crust of the Russian shield (Meissner 1976) but are quite abundant in young orogenic areas like the Alps (Giese 1968, 1970). On the other hand, large parts of mesozoic continental crust with average geotherms seem to have a rather constant velocity over many kilometers in the middle crust.

The pronounced velocity anisotropy in the amphibolite and peridotite rocks measured at high confining pressure and high temperatures, i.e., at conditions of great depth, may account for significant velocity anisotropy reported from deep seismic sounding. Bamford (1977) and Fuchs (1979) measured velocity anisotropy of 7–8% in the continental subcrustal litosphere. Seismic measurements reported by Hess (1964), Francis (1969), and Keen and Barett (1971) indicate anisotropy of the upper mantle under the Pacific Ocean. Velocities averaging 8.3 km/s. perpendicular to mid-ocean ridges contrast with velocities of about 8.0 km/s. parallel to the ridges, corresponding to anisotropy values of about 3.6%. Raitt et al. (1969) observed a large velocity anisotropy of about 7% in the region between California and Hawaii. These seismic anisotropies may be best explained by preferred latice orientation of the constituent minerals in the mantle material (see also Kern and Fakhimi 1975). As shown in this paper and by Kern (1978), elastic anisotropy induced by preferred lattice orientation is unaffected by high pressures and temperatures up to 700° C.

Acknowledgements. We wish to thank R. Meissner (Kiel), H.R. Wenk (Berkeley) and J. Zschau (Kiel) for helpful discussions and critical reading of the manuscript. We are grateful to P.K. Hörmann for oxide analyses and to M. Schroetel for assistance in performing the experiments. Financial support by the Deutsche Forschungsgemeinschaft, Bonn – Bad Godesberg, is gratefully acknowledged.

References

Bamford, D.: *P* velocity anisotropy in a continental upper mantle. Geophys. J. **49**, 29–48, 1977

Birch, F.: The velocity of compressional waves in rocks to 10 kbar, Part 1 J. Geophys. Res. **65**, 1083–1102, 1960

Birch, F.: The velocity of compressional waves in rocks to 10 kbar, Part 2. J. Geophys. Res. **66**, 2199–2224, 1961

Christensen, N.I.: Compressional wave velocities in metamorphic rocks at pressures to 10 kbar. J. Geophys. Res. **70**, 6147–6164. 1965

Christensen, N.I.. Shear-wave velocities in metamorphic rocks at pressures to 10 kbar. J. Geophys. Res. **71**, 3549–3556, 1966

Christensen, N.I.: Compressional wave velocities in possible mantle rocks to pressures of 30 kbar. J. Geophys. Res. **79**, 407–412, 1974

Christensen, N.I.: Compressional wave velocity in rocks at high temperatures and pressures. Critical thermal gradients, and crustal low-velocity zones. J. Geophys. Res. **84**, 6849–6857, 1979

Christensen, N.I., Fountain, D.M.: Constitution of the lower continental crust based on experimental studies of seismic velocities in granulite. Geol. Soc. Am.Bull. **86**, 227–236, 1975

Fielitz, K.. Untersuchungen von Kompressions- und Scherwellengeschwindigkeiten in Gesteinen unter erhöhtem Druck. Geophys. **37**, 943–956, 1971

Francis, T.J.G.: Generation of seismic anisotropy in the upper mantle along the mid-oceanic ridges. Nature **221**, 162–165, 1969

Fuchs, K.: The subcrustal lithosphere – mechanical properties, differentiation and dynamical processes. Tectonophysics **56**, 1–15, 1979

Giese, P.: Die Struktur der Erdkruste im Bereich der Ivrea-Zone. Schweiz. Mineral. Petrogr. Mitt. **48**, 261–284, 1968

Giese, P.: The structure of the earth's crust in central Europe. Proc. 10th Gen. Ass. Europ. Seismol. Comm. (Leningrad 1968), 387–403. Moscow: Acad. Sci. USSR 1970

Hess, H.H.. Seismic anisotropy of the uppermost mantle under oceans. Nature **204**, 629–631, 1964

Keen, C.E., Barett, D.L.: A measurement of seismic anisotropy in the North-East Pacific. Can. J. Earth Sci. **8**, 1056–1064, 1971

Kern, H.. The effect of high temperature and high confining pressure on compressional wave velocities in quartz-bearing and quartz-free igneous and metamorphic rocks. Tectonophysics **44**, 185–203, 1978

Kern, H.. Effect of high-low quartz transition on compressional and shear wave velocities in rocks under high pressure. Phys. Chem. Minerals **4**, 161–167, 1979

Kern, H., Fakhimi, M.: Effect of fabric anisotropy on compressional wave propagation in various metamorphic rocks for the range 20°–700° C at 2 kbars. Tectonophysics **28**, 227–244, 1975

Kern, H., Richter, A.: Compressional and shear wave velocities at high temperature and high confining pressure in basalts from the Faeroe islands. Tectonophysics **54**, 231–252, 1979

Kumazawa, M., Anderson, O.L.: Elastic moduli, pressure derivatives, and temperature derivatives of single-crystal olivine and single-crystal forsterite. J. Geophys. Res. **74**, 5961–5972, 1969

Meissner, R.: Comparison of wide-angle measurements in the USSR and the Federal Republic of Germany. In: Explosion seismology in central europe, P. Giese, C. Prodehl, A. Stein, eds.: pp 380–384. Berlin, Heidelberg, New York: Springer 1976

Nur, A., Simmons, G.: The effect of saturation on velocity in low porosity rocks. Earth Planet. Sci. Lett. **7**, 183–193, 1969

Peselnick, L., Nicolas, A.: Seismic anisotropy in an ophiolite peridotite: application to oceanic upper mantle. J. Geophys. Res. **83**, 1227–1235, 1978

Raitt, R.W., Shor, G.G., Francis, T.J.G., Morris, G.B.. Anisotropy of the Pacific upper mantle. J. Geophys. Res. **74**, 3095–3109, 1969

Ramananantoandro, R., Manghnani, M.H.: Temperature dependence of the compressional wave velocity in an anisotropic dunite: Measurements to 500° C at 10 kbar. Tectonophysics **47**, 73–84, 1978

Simmons, G.: Velocity of shear waves in rocks to 10 kbar. J. Geophys. Res. **69**, 1123, 1964

Spencer, J.W., Jr., Nur, A.M.: The effect of pressure, temperature and pore water on velocities in Westerly granite. J. Geophys. Res. **81**, 899–904, 1976

Stewart, R., Peselnick, L.: Velocity of compressional waves in dry Franciscan rocks to 8 kbar and 300° C. J. Geophys. Res. **82**, 2027–2039, 1977

Stewart, R., Peselnick, L.: Systematic behavior of compressional velocity in Franciscan rocks at high pressure and temperature. J. Geophys. Res. **83**, 831–839, 1978

Theilen, F., Meissner, R.. A comparison of crustal and upper mantle features in Fennoscandia and the Rhenish shield, two areas of recent uplift. Tectonophysics **61**, 227–242, 1979

Received February 21, 1980; Revised Version July 1, 1980
Accepted August 7, 1980